Original Article

Construction and validation of a chromatin regulator-related gene signature for prognostic and therapeutic significance of clear cell renal cell carcinoma

Changzheng Zhang[1#], Jiayi Zeng[2#], Chujin Ye[1], Kaiwen Tian[1], Zhiyong Xian[1,2]

[1]Department of Urology, Guangdong Provincial People's Hospital (Guangdong Academy of Medical Sciences), Southern Medical University, Guangzhou, China; [2]Department of Urology, Guangdong Provincial People's Hospital's Nanhai Hospital, Foshan, China

Contributions: (I) Conception and design: C Zhang, J Zeng; (II) Administrative support: Z Xian; (III) Provision of study materials or patients: J Zeng, C Ye; (IV) Collection and assembly of data: J Zeng, K Tian; (V) Data analysis and interpretation: C Zhang, J Zeng; (VI) Manuscript writing: All authors; (VII) Final approval of manuscript: All authors.

[#]These authors contributed equally to this work.

Correspondence to: Zhiyong Xian, MM. Department of Urology, Guangdong Provincial People's Hospital (Guangdong Academy of Medical Sciences), Southern Medical University, No. 106, Zhongshan 2nd Road, Guangzhou 510080, China; Department of Urology, Guangdong Provincial People's Hospital's Nanhai Hospital, No. 23 Pingzhouxiadong Road, Foshan 528251, China. Email: urologist@163.com.

Background: Epigenetic alterations driven by chromatin regulators (CRs) are well-recognized cancer hallmarks. Growing evidence suggests that the imbalance of CRs may lead to the occurrence of various diseases including tumors. However, the role and prognostic value of CRs in clear cell renal cell carcinoma (ccRCC) remain undefined.

Methods: Consensus clustering analysis was used to identify different subtypes. Univariate and multivariate Cox regression analysis were performed to identify prognosis-related CRs and constructed a risk model. Transcriptome sequencing was used to verify gene expression levels. Kaplan-Meier survival analysis was used to compare overall survival (OS) between high- and low-risk groups. The area under the curve (AUC) value of the receiver operating characteristic (ROC) curve was used to evaluate the performance of the model. The ESTIMATE algorithm and single-sample gene set enrichment analysis (ssGSEA) were executed to evaluate the immune characteristics of samples. Correlation analysis was used to assess the relationship between risk score and immune checkpoint genes, the relationship between expression levels of CRs and immune cell infiltration and drug therapeutic response. Finally, we also compared differences in drug sensitivity between low- and high-risk groups.

Results: We identified three CRs-related subtypes with different characteristics. A prognostic model was built with four CRs and can precisely predict the OS of patients in different risk groups. The model has good stability and applicability and was further verified in the internal and external dataset. The transcriptomic levels of the four CRs were also validated, and the risk score was an independent prognostic factor for ccRCC. Obvious differences in the immune microenvironment and the expression levels of immune checkpoints were observed in low- and high-risk group. Higher immune activity and immune cell infiltration were found in the high-risk group. Besides, the expression levels of CRs were associated with drug therapeutic response. Patients with high-risk score may be more sensitive to gemcitabine, vinblastine, paclitaxel, axitinib, sunitinib, and temsirolimus.

Conclusions: CRs were strongly associated with the occurrence and development of ccRCC. Targeting CRs may become a new therapeutic strategy for ccRCC. Besides, CRs-related gene signature can predict the prognosis and therapeutic significance of ccRCC, which provides an important reference for clinical decision-making.

Keywords: Gene signature; prognosis; therapeutic response; clear cell renal cell carcinoma (ccRCC)

Submitted Aug 03, 2023. Accepted for publication Nov 29, 2023. Published online Jan 15, 2024.
doi: 10.21037/tcr-23-1383
View this article at: https://dx.doi.org/10.21037/tcr-23-1383

Introduction

As a popular malignant tumor in urinary system, the incidence of renal cell carcinoma (RCC) is increasing year by year (1). Every year, there are approximately 431,000 new cases of RCC worldwide, resulting in more than 179,000 deaths (2). Clear cell renal cell carcinoma (ccRCC) is considered as the deadliest and the most common histological type, accounting for more than 80% of RCC (3). The ccRCC has relatively specific immunological features, including high immune infiltration and low tumor mutational burden (TMB), resistance to chemotherapy, and relative sensitivity to antiangiogenic and immunotherapy (4). It is insensitive to conventional chemotherapy and radiotherapy, and nephrectomy, targeted therapy and immunotherapy are the main therapies for ccRCC (5-7). However, about 30% of ccRCC patients have distant metastases at the first diagnosis. Around 30–40% of patients with the early-stage or localized disease even having undergone surgical resection will develop metastatic recurrence during follow-up (8). Although significant progress has been made in targeted therapy and immunotherapy, the overall survival (OS) is still not satisfactory in advanced or metastatic patients (9). Low response rates to immunotherapy also limit its therapeutic efficacy (10). Considering the limitations of ccRCC treatment and bad prognosis of advanced patients, we need to explore new therapeutic targets to improve the prognosis.

The continuous development of bioinformatics provides convenience for exploring the biomarkers of tumors. Chen *et al.* (11) found SPOCK1 participates in the epithelial-mesenchymal transition process and may be a potential prognostic biomarker in ccRCC. Shao *et al.* (12) found that the down-regulation of ALDOB was closely related to the clinicopathological features, poor prognosis, immune infiltration and m6A modification of ccRCC patients by integrating multiple public databases. Liao *et al.* (13) established a survival and prognosis model system by exploring immune-related genes, and provided an effective prediction tool for the future. Zhou *et al.* (14) not only used data analysis, but also supplemented immunohistochemical staining and cell line experiments, which proved that high expression of CD73 contributes to poor prognosis of ccRCC by promoting cell proliferation and migration. These findings are good supplement to the study of ccRCC biomarkers. Identifying novel biomarkers and exploring risk prediction models to optimize treatment strategies remain important tasks in precision medicine.

Epigenetic alterations are driven by chromatin regulators (CRs), which are currently recognized hallmarks of cancer (15). CRs have been shown to be the indispensable upstream regulators of epigenetics (16). CRs play distinct regulatory effect in epigenetics, which are commonly classified into three types: DNA methylators, histone modifiers, and chromatin remodelers (17-19). Previous research has shown that the dysregulation of CRs is closely involved in many biological processes, including inflammation, autophagy, apoptosis, and proliferation (20-23). Further exploration revealed that mutations and dysregulation of CRs contribute to tumorigenesis, heterogeneity of tumor, and drug resistance (24-28). CCCTC-binding factor (CTCF) is a transcriptional regulator and uniquely participates in regulation of epigenetic, including the regulation of cancer-specific genes and cell cycle (29,30). Damaschke *et al.* (31) found that dysregulation of chromodomain helicase DNA-

Highlight box

Key findings

- Chromatin regulators (CRs) were strongly associated with the occurrence and development of clear cell renal cell carcinoma (ccRCC).

What is known and what is new?

- CRs have been shown to be the indispensable upstream regulators of epigenetics. The mutations and dysregulation of CRs contribute to tumorigenesis, heterogeneity of tumor, and drug resistance.
- In this study, we constructed a prognostic prediction model based on four CRs, which can precisely predict the prognosis of ccRCC patients. Additionally, significant differences between different groups of patients regarding immune microenvironment, immune checkpoints, immune cell infiltration, and immune activity were observed. The expression levels of CRs are associated with drug therapeutic response. Patients in different groups have different susceptibility to common anticancer drugs.

What is the implication, and what should change now?

- CRs-related gene signature can predict the prognosis and drugs therapeutic significance of ccRCC.

binding protein 8 (CHD8) and CTCF leads to abnormal chromatin structure and epigenetic alterations in cancer-related genes, ultimately leading to prostate cancer progression and poor prognosis. Chromobox 7 (CBX7) is considered as a tumor suppressor gene, which can inhibit the progression of bladder cancer by down-regulating AKR1B10 and further inactivating ERK signaling (32). Furthermore, high mRNA levels of CBX7 in ovarian clear cell adenocarcinoma tissues usually indicate a bad prognosis (33). Enhancer of zeste homolog 2 (EZH2) is a vital epigenetic regulator and EMT inducer, which was found to be strongly associated with the metastasis of multiple cancers (34). Zhang *et al.* (35) found that EZH2 can promotes osteolytic metastasis of breast cancer through regulating transforming growth factor beta (TGFβ) signaling. Besides, the high expression levels of EZH2 were also involved in invasiveness of prostate cancer, cutaneous melanoma, and endometrial cancer and promotes disease progression to the advanced stage (36-39). Expression of HX family members is also thought to correlate with cancer progression and survival time. Zinc fingers and homeoboxes 2 (ZHX2), a potent inhibitor of cyclins A and E expression, can inhibit cell proliferation in hepatocellular carcinoma (HCC) and reduce xenograft tumor growth in mice (40). Decreased expression of zinc fingers and homeoboxes 1 (ZHX1) and zinc fingers and homeoboxes 3 (ZHX3) is associated with advanced pathological stages and poor OS of ccRCC (41). A variety of biological functions are controlled by WD repeat domain 5 (WDR5) via epigenetic regulation of gene expression. It has been found that WDR5 can promote the tumorigenesis of oral squamous cell carcinoma (42) and is closely related to the immune escape of pancreatic cancer (43). These studies have demonstrated that CRs contribute to tumorigenesis and progression.

Yet, only a few studies have been conducted on the specific functions of CRs in ccRCC. The role and prognostic value of CRs in ccRCC remain unclear. We speculate that CRs may play a tumor-promoting role in ccRCC and is related to the prognosis of patients. In this research, we investigated the expression profile and the prognostic value of CRs in ccRCC based on bioinformatics approaches, as well as its impacts on tumor microenvironment (TME) and therapeutic response. This provides new ideas and insights for predicting the prognosis of ccRCC patients and developing possible treatment strategies. We present this article in accordance with the TRIPOD reporting checklist (available at https://tcr.amegroups.com/article/view/10.21037/tcr-23-1383/rc).

Methods

Data collection and processing

Transcriptome information and clinicopathological features of 539 cases of ccRCC and 72 cases of normal renal tissues were obtained from the Cancer Genome Atlas (TCGA) database (https://portal.gdc.cancer.gov/repository). The somatic mutation data of ccRCC can also be found in the TCGA database. ArrayExpress database (https://www.ebi.ac.uk/biostudies/arrayexpress) provides transcriptomic and clinical information of the E-MTAB-1980 cohort (101 ccRCC cases). A total of 870 CRs were obtained from previously published research (16). In addition, we obtained 318 tumor-associated transcription factors (TFs) from the Cistrome cancer database (http://cistrome.org/CistromeCancer/). The information of 507 ccRCC samples was obtained after integrating CR transcriptional data and survival information (survival time >30 days) in the TCGA dataset. Then, a ratio of 7 to 3 was executed to stochastically divide the patients into a training cohort and a testing cohort. The flowchart of the study is shown in Figure S1.

Identification of differentially expressed CRs in ccRCC

The mNRA levels of all CRs were firstly extracted from the TCGA dataset and the E-MTAB-1980 dataset, which were normalized by R packages to reduce the effects of the batch effect. The "limma" R package was then executed to identify the differentially expressed CRs between ccRCC and normal renal tissues in the TCGA dataset with the set threshold was |log fold change (FC)| >1 and false discovery rate (FDR) <0.001. Next, the same method was performed to examine the differentially expressed TFs between tumor and normal tissues. The protein-protein interaction (PPI) network of these CRs was obtained via the STRING database (https://cn.string-db.org/cgi/input). Univariate Cox regression analysis was executed on CRs to evaluate their prognostic value, and a prognostic network was presented via the corresponding R package. The correlation analysis was executed to establish a regulatory network between prognosis-related CRs and differentially expressed TFs (cor >0.6 and P value <0.001) and visualized in Cytoscape.

Consensus clustering analysis of differentially expressed CRs

We performed consensus cluster analysis through the

R package "ConsensusClusterPlus" to identify different subtypes according to the expression of differentially expressed CRs. We think it is the best result when the subtype number k=3. Subsequently, functional enrichment analysis was used to investigate the biological function differences of CRs in different subtypes, including Gene Ontology (GO) analysis and Kyoto Encyclopedia of Genes and Genomes (KEGG) pathway analysis, and FDR <0.05 was considered to be meaningful results.

Association of CR-related subtypes with prognosis and clinicopathological features

We compared the differences of clinical features and prognosis among different subtypes to judge the clinical value of CR-related subtypes derived from consensus clustering analysis. The clinical characteristics of patients included survival status, gender, age, Tumor Node Metastasis (TNM) stage, grade, and the American Joint Committee on Cancer (AJCC) stage. The differences in OS and progression-free survival (PFS) among different subtypes were examined by the Kaplan-Meier curves.

Construction and validation of a CR-related prognostic model

We executed multivariate Cox regression analysis on the prognosis-related CRs obtained by above analysis to distinguish independent prognostic factors. Then, a risk prognostic model was built in training cohort. Using the following formula to count patient's risk score:

$$\text{Risk score} = \sum(\text{Ci} \times \text{Ei}) \quad [1]$$

where Ci represented the risk coefficient and Ei represented mRNA levels of each gene. Patients in the training cohort were divided into low- and high-risk group on the basis of the median value of risk score. The difference in prognosis between two groups was compared by Kaplan-Meier curves produced by survival analysis. The efficiency of the model was judged according to the area under the curve (AUC) values corresponding to the receiver operating characteristic (ROC) curves. On the basis of the "ggplot2" R package, we performed the T-distributed stochastic neighbor embedding (t-SNE) analysis to determine the ability of the model to discriminate patients in different groups. The testing cohort, TCGA entire cohort, and E-MTAB-1980 external cohort were as validation datasets to further confirm the predictive capability of the model.

Clinical correlation, independent prognostic analysis and stratification analysis of the model

Chi-squared test was executed to assess the correlation between clinical features and risk score, including patient's age, gender, T stage, M stage, grade, and AJCC stage. Univariate and multivariate Cox risk regression analyses were subsequently used to evaluate the impact of clinical characteristics and risk score on ccRCC. Besides, we conducted a stratification analysis to assess whether the model maintained predictive performance in different clinical subgroups.

TME and immune checkpoints

We calculated the TME scores for all samples through the ESTIMATE algorithm to assess the difference in the TME between two groups. The CIBERSORT algorithm was executed to quantify the infiltrating levels of 22 human immune cells in ccRCC samples. Then, correlation test was performed to evaluate the relevance between risk score and immune cells. The single-sample gene set enrichment analysis (ssGSEA) was run to estimate the infiltration fraction of 16 immune cells and the activity of 13 immune-related pathways among two groups. Furthermore, the expression levels of common immune checkpoint between two groups were also analyzed in this study.

Gene Set Enrichment Analysis (GSEA)

GSEA was run based on the gene set c2.cp.kegg.v7.4.symbols.gmt derived from the MSigDB database (http://www.broad.mit.edu/gsea/msigdb/, c2.cp.kegg.v7.4.symbols.gmt) to further explore the potential molecular mechanism of the difference between two group. FDR ≤0.25 and P values <0.05 were considered a significant enrichment criterion.

Somatic mutation and drug sensitivity analysis

We used the waterfall diagram generated by the "maftools" R package to evaluate the frequency of somatic mutations between two groups. We downloaded the NCI-60 data from the CellMiner platform (https://discover.nci.nih.gov/cellminer/home.do), including the efficacy of common anticancer drugs and gene expression information of cancer cells. Correlation test was carried out to evaluate the relationship between the expression levels of CRs and

therapeutic response. The semi-inhibitory concentration (IC50) values of drugs were estimated via the "pRRophetic" R package for exploring the difference in sensitivity to common anticancer drugs among two groups, and P value <0.05 was considered statistically significant.

Tissue samples and transcriptome sequencing

A total of 18 tumor samples and 6 paracancerous samples were collected from 6 ccRCC patients treated at Guangdong Provincial People's Hospital, and the specimens were cryopreserved in liquid nitrogen for subsequent transcriptome sequencing. The pathology of the patient's postoperative tumor specimen was reviewed and determined to be ccRCC by two independent pathologists. According to the manufacturer's agreement, transcriptome sequencing was performed for each case of ccRCC tissue and matched with paracancerous samples. The study was conducted in accordance with the Declaration of Helsinki (as revised in 2013). The study was approved by the Ethics Committee of Guangdong Provincial People's Hospital (IRB number: KY-Z-2021-657-01) and informed consent was obtained from all individual participants.

Statistical analysis

The Wilcoxon test was conducted to compare the differences between two groups. The Chi-squared test was run for the comparison of categorical variables. All R packages and statistical analysis methods were execucating that CRs may p0.4). All the results of statistical analyses are two-sided, the AUC values of the model greater than 0.5 and P value less than 0.05 was considered to be meaningful results.

Results

Differentially expressed CRs in ccRCC

A total of 89 differentially expressed CRs were identified in the TCGA-KIRC dataset compared to normal tissue, including 58 up-regulated CRs and 31 down-regulated CRs. *Figure 1A*,*1B* shows their expression heatmap and volcano plot. In order to analyze the interaction of these CRs, we used the STRING database to set the lowest interaction score to 0.9 (the highest confidence), and finally obtained their PPI network excepting isolated genes (*Figure 1C*). Based on these dysregulated CRs, we executed a univariate Cox prognostic analysis to assess their predictive value (*Figure 1D*). The prognostic network showed more intuitively correlation among these CRs and their relationship with prognosis (*Figure 1E*). In addition, we also identified 60 differentially expressed TFs in normal kidney tissue and ccRCC (*Figure 1F*). The interaction between TFs and genes is an important way to regulate gene transcription. In tumor tissue, their regulatory relationship may undergo major changes. So, we constructed a network of possible regulatory relationships between CRs and TFs (*Figure 1G*), which provides possible predictions for further research on the mechanisms of CRs and tumorigenesis or inhibition.

CR-related subtypes in ccRCC

To investigate the correlation between different subtypes and expression levels of CRs, we performed the consensus clustering analysis on differentially expressed CRs using the "ConsensusClusterPlus" R package. We think it is the best classification subtypes when the subtype number k=3, and finally determine three CR-related subtypes (C1, C2, and C3) (*Figure 2A-2C*). Kaplan-Meier survival curve was utilized for comparing the survival differences among three subtypes. The results showed the strong differences in OS and PFS among the three subtypes. The subtype C3 had the best prognosis, followed by subtype C1, and subtype C2 had the worst prognosis (*Figure 2D*,*2E*, P<0.001). The obvious differences were also found in survival status, TNM stage, grade, and AJCC stage among three subtypes (P<0.001), but meaningless difference in age (*Figure 2F*). Specifically, subtype C2 was more common in men and had bad grade, AJCC stage, and TNM stage. The patients with subtype C2 showed high expression of CRs as a whole, and the proportion of deaths was the highest, indicating that CRs are strongly involved in the tumorigenesis and prognosis of ccRCC. In addition, we further excavated the biological function differences of CRs in different subtypes through functional enrichment analysis. Immune-related biological processes were discovered by GO enrichment analysis, such as B cell-mediated immunity, complement activation, lymphocyte-mediated immunity, etc. (*Figure 2G*). KEGG enrichment analysis showed significant enrichment in pathways such as cytokine-cytokine receptor interaction, protein digestion and absorption, cell cycle, p53 signaling pathway etc. (*Figure 2H*).

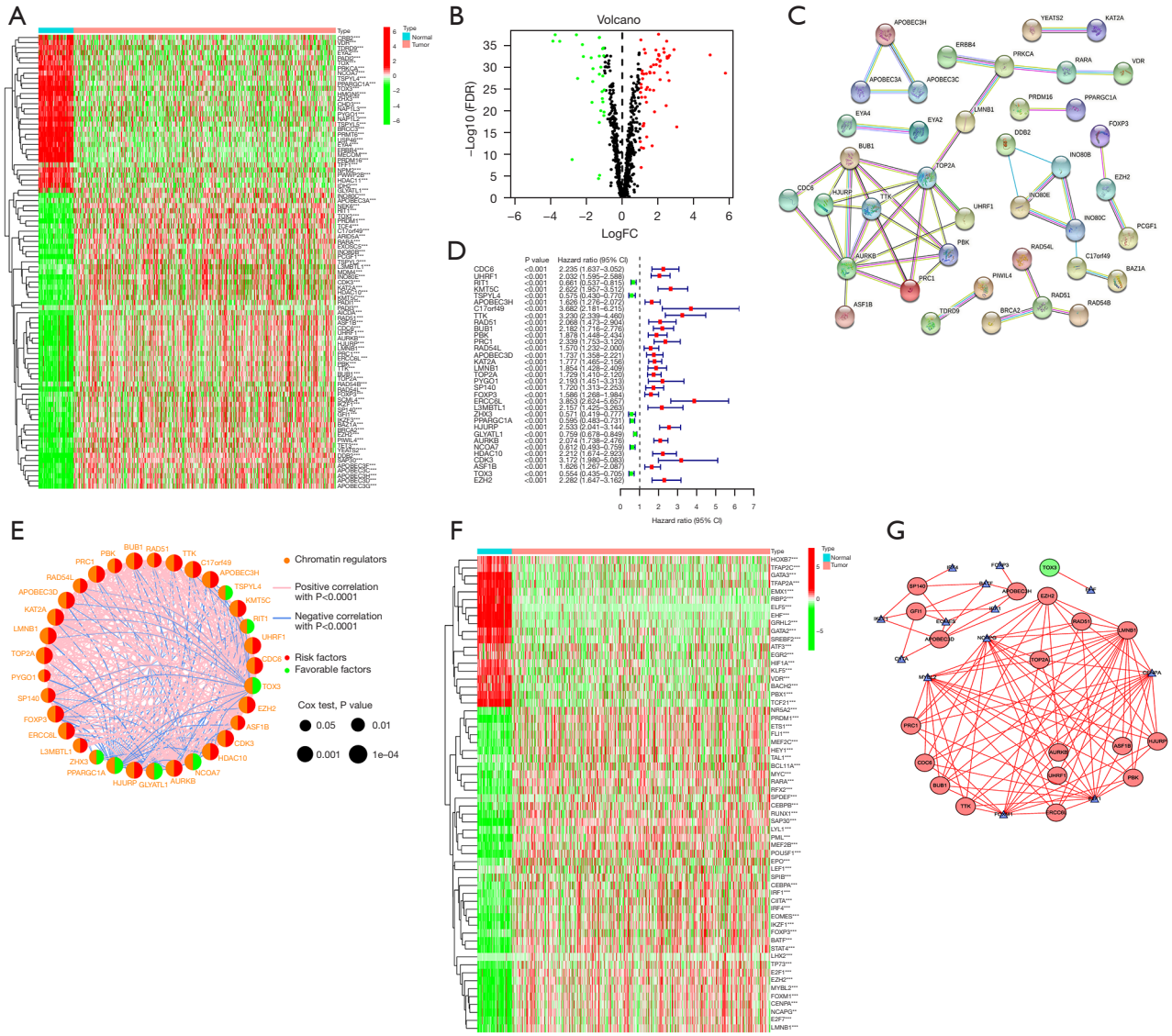

Figure 1 Identification of differentially expressed CRs in ccRCC. (A,B) The expression heatmap and volcano plot of 89 differentially expressed CRs. Red dots indicate genes whose expression is up-regulated, green dots indicate genes whose expression is down-regulated, and black dots indicate genes whose expression is not significantly different. (C) The PPI network of differentially expressed CRs. (D) The result of univariate Cox prognostic analysis on differentially expressed CRs. (E) The prognostic network of 33 CRs. The line connecting the CRs represents their interaction, blue and pink represent negative and positive correlations, respectively. (F) The expression heatmap of 60 differentially expressed TFs. (G) The regulatory network of TFs and CRs. **, P<0.01; ***, P<0.001. FDR, false discovery rate; FC, fold change; CI, confidence interval; CRs, chromatin regulators; ccRCC, clear cell renal cell carcinoma; PPI, protein-protein interaction; TFs, transcription factors.

A CR-related prognostic model

Multivariate Cox regression analysis was performed on prognosis-related CRs to judge their independent prognostic value for the prognosis of ccRCC patients. Finally, four CRs with independent prognostic value, including TTK, L3MBTL1, glycine-N-acyltransferase-like 1 (GLYATL1) and TOX3, were identified for predicting OS, and a risk prognostic model was established in the training cohort. Among them, TTK and L3MBTL1 were

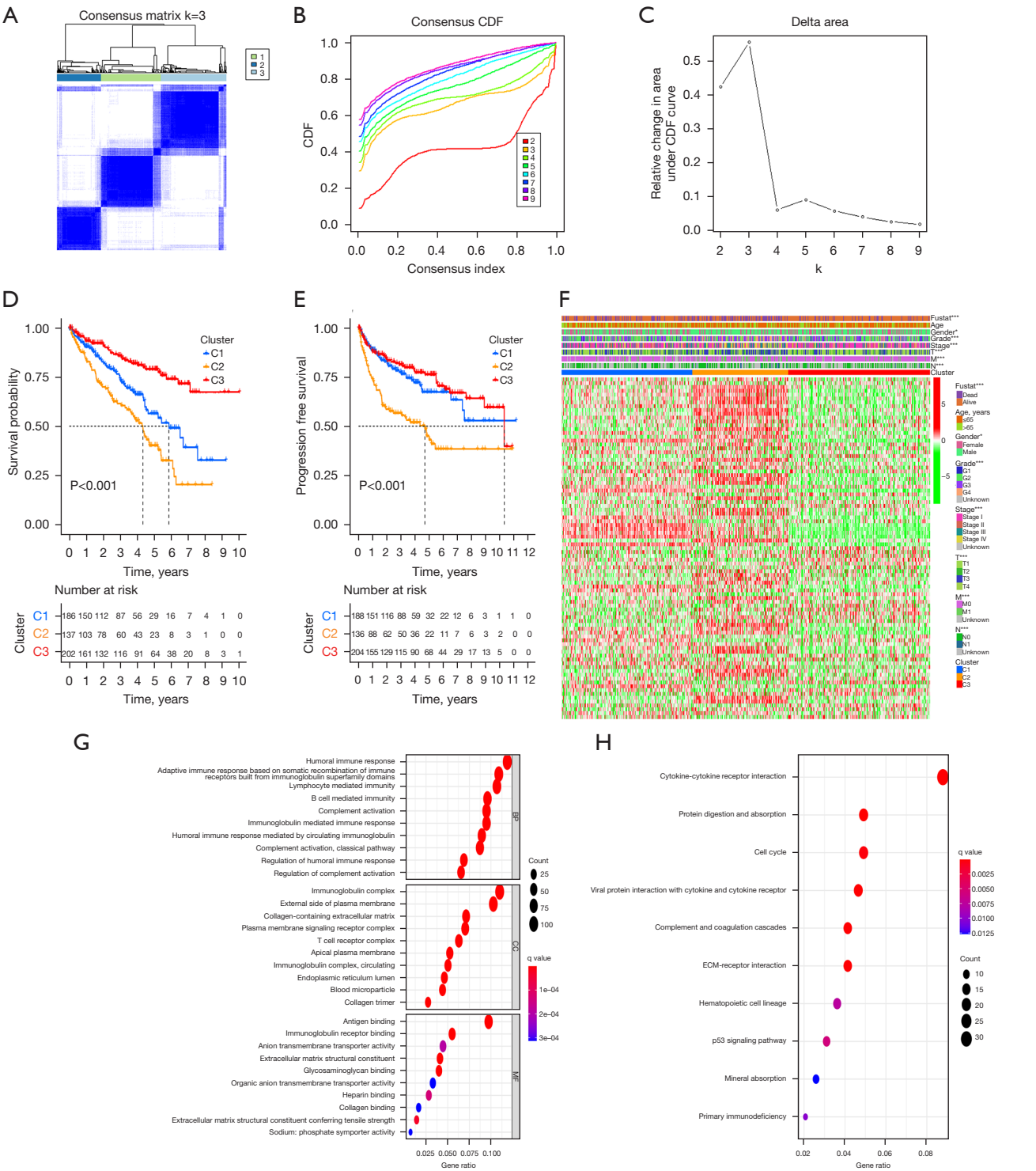

Figure 2 Identification of CR-related subtypes in ccRCC. (A-C) Consensus matrix heatmap defining three clusters (k=3) and CDF curve and relative change in area under the CDF curve. (D,E) A comparison of survival curves of patients with ccRCC between three subtypes according to Kaplan-Meier analysis. (F) The differences of clinical features and the expression levels of CRs among three subtypes. (G) The results of GO enrichment analysis. (H) The results of KEGG enrichment analysis. *, P<0.05; ***, P<0.001. CDF, cumulative distribution function; CR, chromatin regulator; ccRCC, clear cell renal cell carcinoma; GO, Gene Ontology; KEGG, Kyoto Encyclopedia of Genes and Genomes; BP, biological process; CC, cellular component; MF, molecular function.

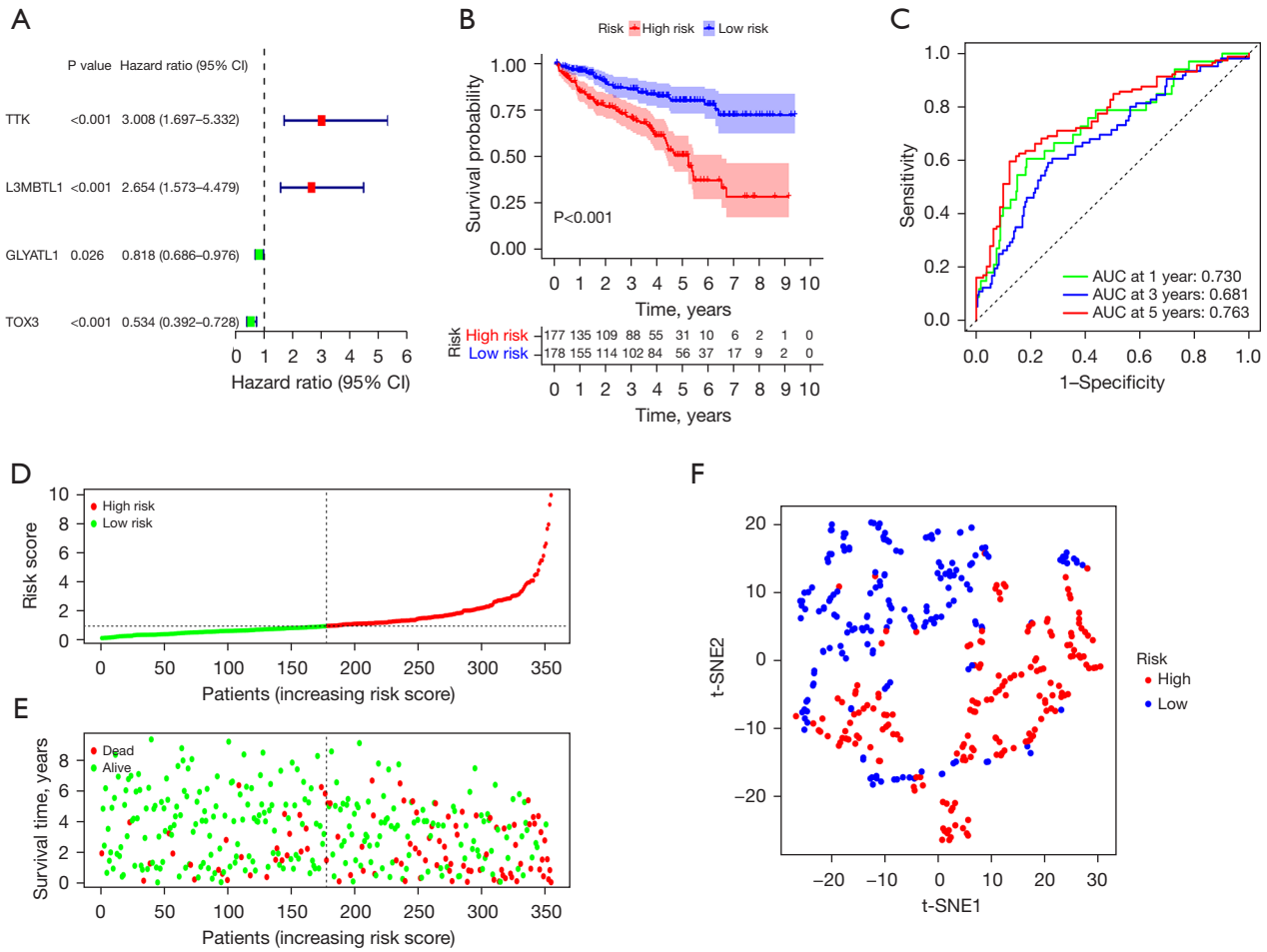

Figure 3 Construction of a CR-related prognostic model. (A) The four CRs with independent prognostic value were identified. (B) Kaplan-Meier survival curves for OS of patients with ccRCC between the low- and high-risk group. (C) The ROC curves of 1-, 3-, and 5-year survival rates according to the prognostic model. (D,E) The risk distribution curve and survival status of patients. (F) The results of the t-SNE analysis. CI, confidence interval; AUC, area under the curve; t-SNE, T-distributed stochastic neighbor embedding; CR, chromatin regulator; OS, overall survival; ccRCC, clear cell renal cell carcinoma; ROC, receiver operating characteristic.

identified as risk genes, and GLYATL1 and TOX3 were identified as favorable genes (*Figure 3A*).

$$\text{Risk score} = (1.101 \times \text{TTK mRNA}) + (0.976 \times \text{L3MBTL1 mRNA}) + (-0.201 \times \text{GLYATLA mRNA}) + (-0.627 \times \text{TOX3 mRNA}) \quad [2]$$

The patients with high-risk score had a poor OS according to Kaplan-Meier survival analysis (*Figure 3B*, P<0.001). The AUC value of the risk prognostic model at 1-, 3-, and 5-year were 0.730, 0.681, and 0.763, respectively, revealing its excellent prediction performance (*Figure 3C*). Furthermore, the survival time of patients decreased and death rate increased significantly with the risk score increased, indicating the negative correlation between prognosis and risk score (*Figure 3D,3E*). The result of the t-SNE analysis showed the good ability of the model to distinguish patients with different risks (*Figure 3F*).

Validation of the prognostic model

We validated the risk prognostic model in the testing cohort, TCGA entire cohort, and E-MTAB-1980 external cohort. Survival analysis showed that patients with high-risk score had shorter OS in testing cohort and TCGA entire cohort, compared to patients with low-risk score (*Figure 4A,4B*, P<0.001). In testing cohort, the AUC value of the ROC curve of the prognostic model at 1-, 3-, and 5-year

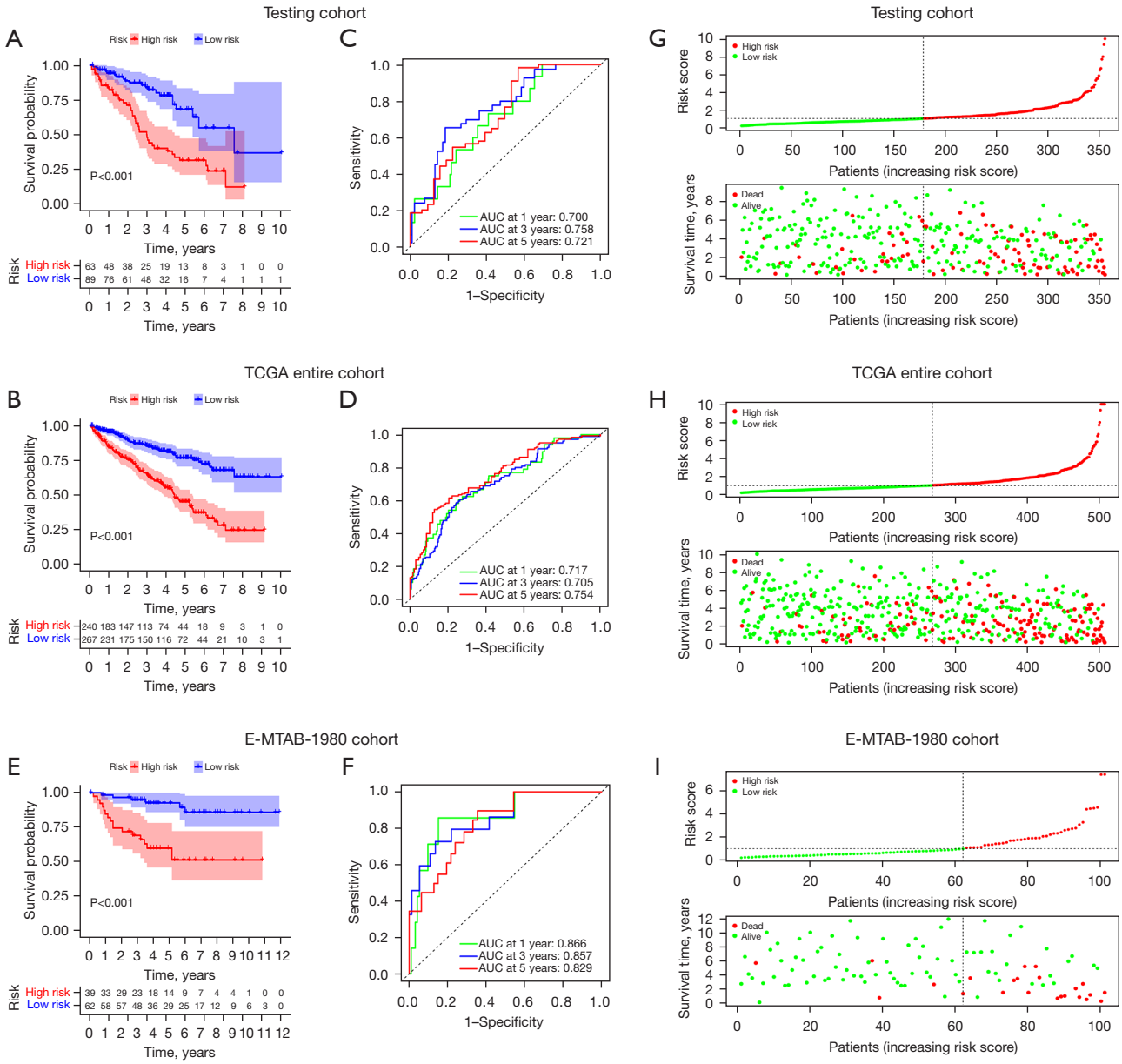

Figure 4 Validation of the prognostic model in internal and external cohorts. (A,B) The Kaplan-Meier survival curves of the two groups in the testing cohort and TCGA entire cohort. (C,D) The ROC curves of 1-, 3-, and 5-year survival rates in the testing cohort and TCGA entire cohort. (E) Kaplan-Meier survival curves between the low- and high-risk group in the E-MTAB-1980 cohort. (F) The ROC curves of 1-, 3-, and 5-year survival rates in the E-MTAB-1980 cohort. (G-I) The risk distribution curve and survival status of patients of three cohorts. AUC, area under the curve; TCGA, The Cancer Genome Atlas; ROC, receiver operating characteristic.

were 0.700, 0.758, and 0.721, respectively (*Figure 4C*). In TCGA entire cohort, the AUC value of the prognostic model at 1-, 3-, and 5-year were 0.717, 0.705, and 0.754, respectively (*Figure 4D*). Besides, consistent with the results of TCGA cohort, patients with high-risk score also had poor OS in E-MTAB-1980 external cohort (*Figure 4E*, P<0.001). The AUC value of the model for predicting OS at 1-year, 3-year, and 5-year were 0.866, 0.857, and 0.829, respectively, showing its excellent predictive performance (*Figure 4F*). The risk distribution curves of the three cohorts also revealed the negative correlation of risk score and prognosis (*Figure 4G-4I*). These data reveal the accuracy of

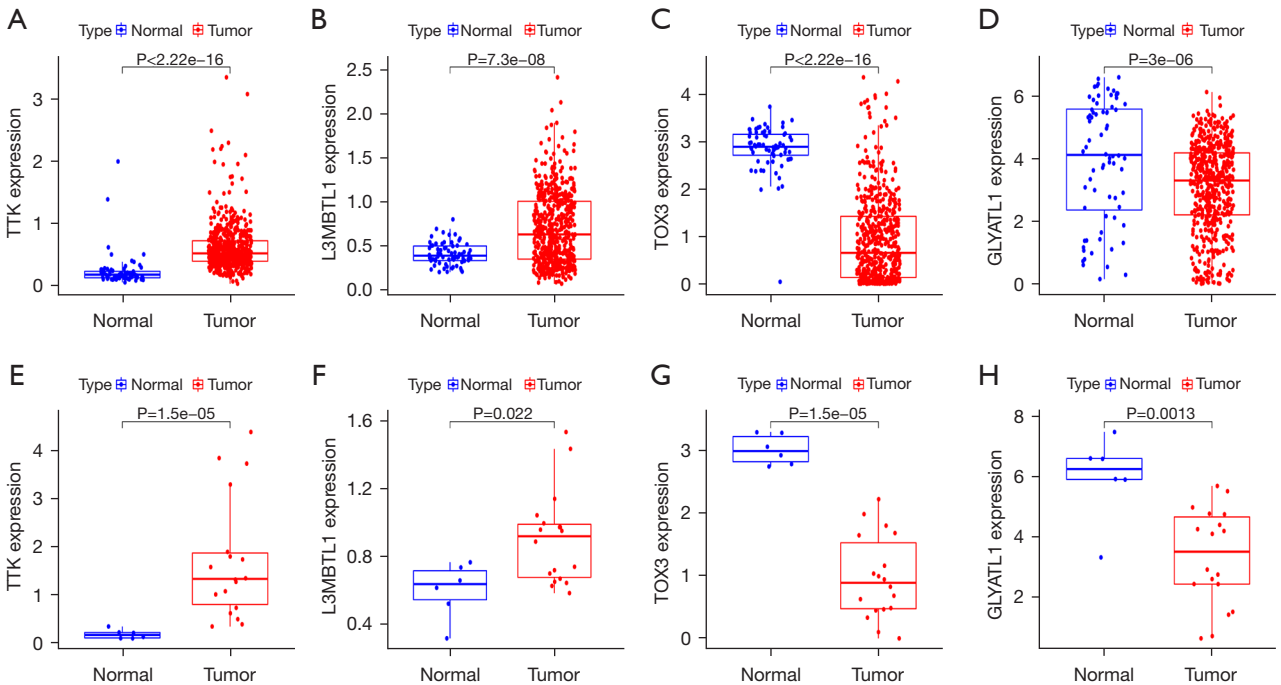

Figure 5 Validation of the mRNA levels of the four CRs used to construct the model. (A-D) The mRNA levels of the four CRs in the TCGA dataset. (E-H) The mRNA levels of the four CRs by high-throughput sequencing. CRs, chromatin regulators; TCGA, The Cancer Genome Atlas.

the risk prognostic model for predicting the prognosis of ccRCC patients.

Validation of the mRNA levels of four CRs

We validated the mRNA levels of four CRs by high-throughput sequencing of 18 tumor samples and 6 paracancerous samples collected. The *Figure 5A-5D* shows the mRNA levels of the four CRs in TCGA dataset. The same results were observed in sequencing data, TTK and L3MBTL1 were highly expressed in ccRCC, and GLYATL1 and TOX3 were lowly expressed in ccRCC (*Figure 5E-5H*).

Risk score was an independent prognostic factor for ccRCC

To estimate the independent prognostic value of the risk score constructed by the four CRs, univariate and multivariate Cox regression analyses were carried out. The results showed that patient's age, grade, AJCC stage, T stage, M stage, and risk score were independent factors for poor survival in ccRCC (*Figure 6A*, P<0.001). Age, grade, AJCC stage and risk score were still considered as independent prognostic indicators for ccRCC after removing interference between confounding factors using multivariate Cox regression analysis (*Figure 6B*, P<0.01). In addition, we also obtained consistent results in E-MTAB-1980 external cohort (*Figure 6C,6D*, P<0.001). These results suggest that the risk score constructed by four CRs was an independent prognostic risk factor for ccRCC.

Relationship between prognostic model and clinical features

To evaluate the effect of risk score on clinical features, we used Chi-square test to judge whether the gene signature based on four CRs was related to the tumorigenesis and progress of ccRCC. Obvious differences in gender (P<0.01), grade (P<0.001), AJCC stage (P<0.001), T stage (P<0.001), and M stage (P<0.001) between high- and low-risk groups were found, but insignificant difference in age (*Figure 7A*). Specifically, high-risk score was related to terminal grade, T stage, M stage, and AJCC stage. Male patients also had higher risk score than female patients (*Figure 7B*). Furthermore, stratification analysis demonstrated that compared with low-risk group, patients with high-risk score had a significantly poorer OS in all

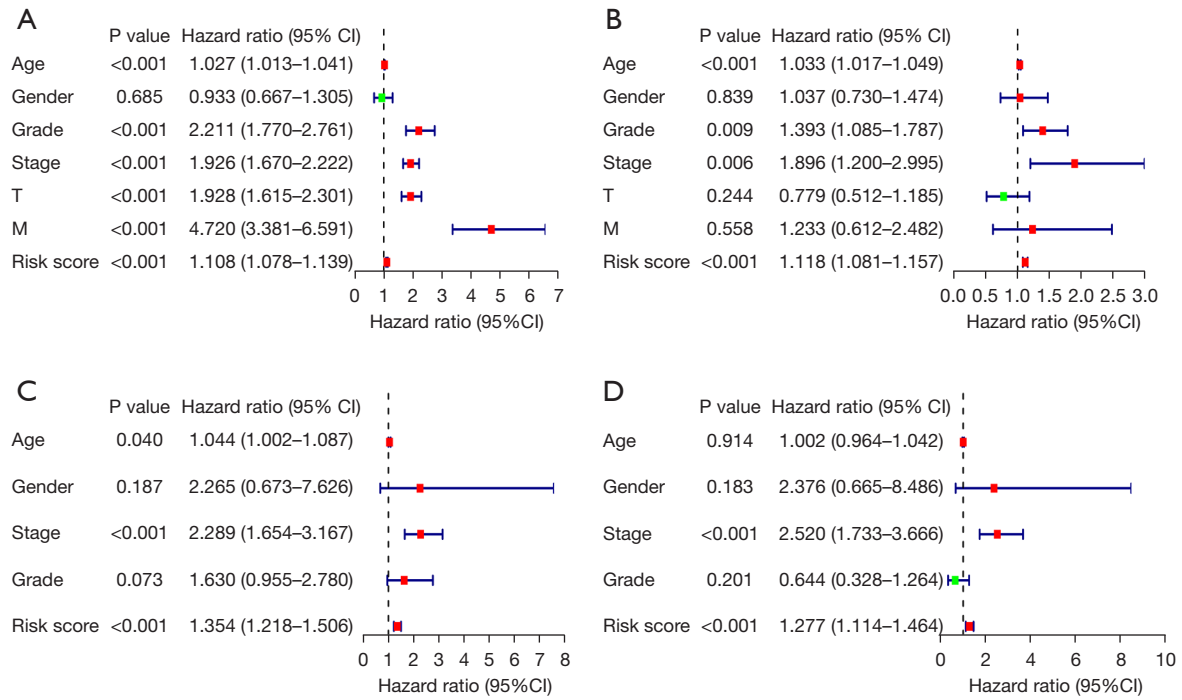

Figure 6 Risk score based on four CRs was an independent prognostic factor for ccRCC. (A) The results of univariate regression analysis of risk score and clinicopathological characteristics for OS in the TCGA dataset. (B) The results of multivariate regression analysis of risk score and clinicopathological characteristics for OS in the TCGA dataset. (C) The results of univariate regression analysis of risk score and clinicopathological characteristics for OS in the E-MTAB-1980 cohort. (D) The results of multivariate regression analysis of risk score and clinical features for OS in the E-MTAB-1980 cohort. CI, confidence interval; CRs, chromatin regulators; ccRCC, clear cell renal cell carcinoma; OS, overall survival; TCGA, The Cancer Genome Atlas.

subgroups except those age >65 years (*Figure 8*). These results showed good applicability and reliable prediction value of the risk model.

Functional enrichment analysis and immune characteristics between low-and high-risk groups

The results of GSEA showed that alpha linolenic acid metabolism, NOD-like receptor signaling pathway, primary immunodeficiency, chemokine signaling pathway, cytokine-cytokine receptor interaction, systemic lupus erythematosus, and taste transduction were significantly enriched in the high-risk group, while oxidative phosphorylation, fatty acid metabolism, PPAR signaling pathway, drug metabolism cytochrome p450, retinol metabolism, tight junction, valine leucine, and isoleucine degradation were majorly enriched in the low-risk group (*Figure 9A*,*9B*). The results of the ESTIMATE algorithm revealed significant difference in TME score between two groups, and high-risk group had higher immune score and stromal score (*Figure 9C*). Correlation analysis showed that the four CRs used to construct the model were closely related to most immune cells (*Figure 9D*). The results of the ssGSEA showed higher levels of immune cell infiltration in the high-risk group, especially $CD8^+$ T cells, macrophages, plasmacytoid dendritic cells (pDCs), regulatory T cells (Treg), tumor infiltrating lymphocytes (TIL), T helper cells, T follicular helper cells (Tfh), Th1 cells, and Th2 cells (*Figure 9E*). Moreover, higher immune activity was also found in the high-risk group. Except for the type II interferon response, the activity of other nine kind immune pathways was higher in the high-risk group (*Figure 9F*). Finally, we compared the expression levels of common immune checkpoint genes among the two groups. Thirty-six immune checkpoints were differentially expressed between low- and high-risk group. And most of them were up-expressed in the high-risk group, including CTLA-4, LAG3, PD-1, PD-L1, etc. (*Figure 9G*).

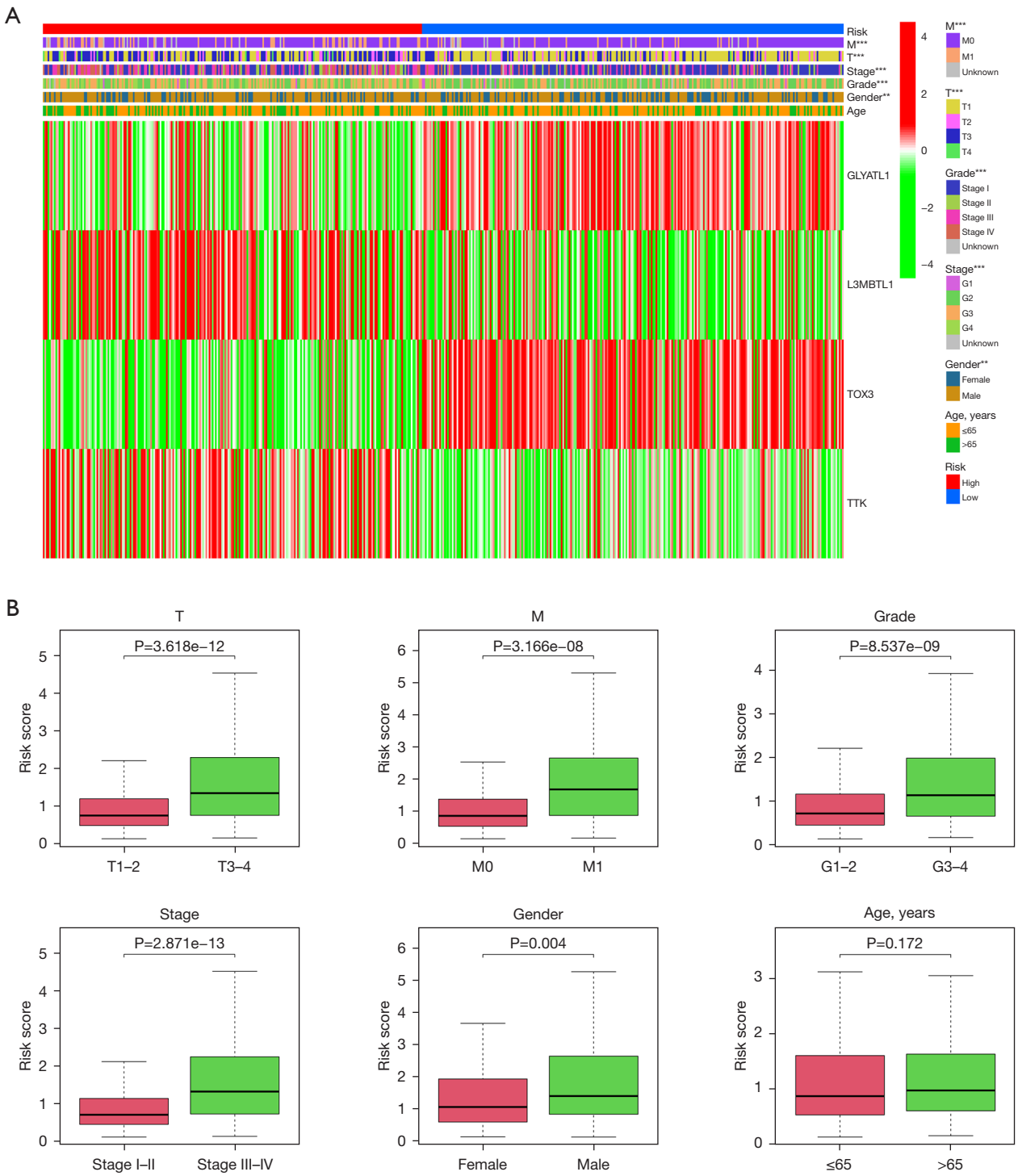

Figure 7 Correlation between prognostic model and clinical features. (A) The heatmap of the difference in risk score. (B) The relationship between risk score and clinical features. **, P<0.01; ***, P<0.001.

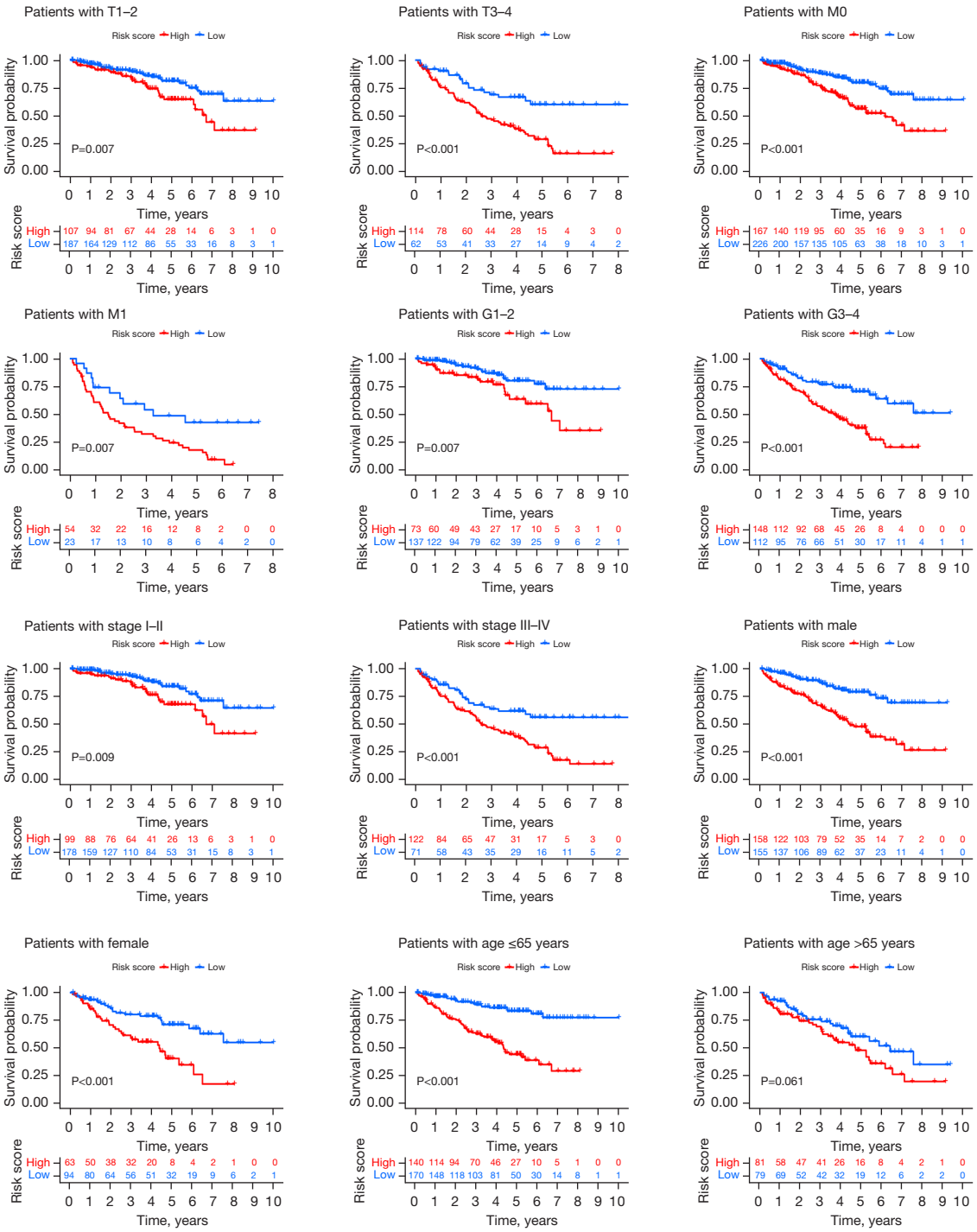

Figure 8 The Kaplan-Meier survival curves of OS differences stratified by age, gender, grade, AJCC stage, T stage, and M stage between the high- and low-risk groups. OS, overall survival; AJCC, American Joint Committee on Cancer.

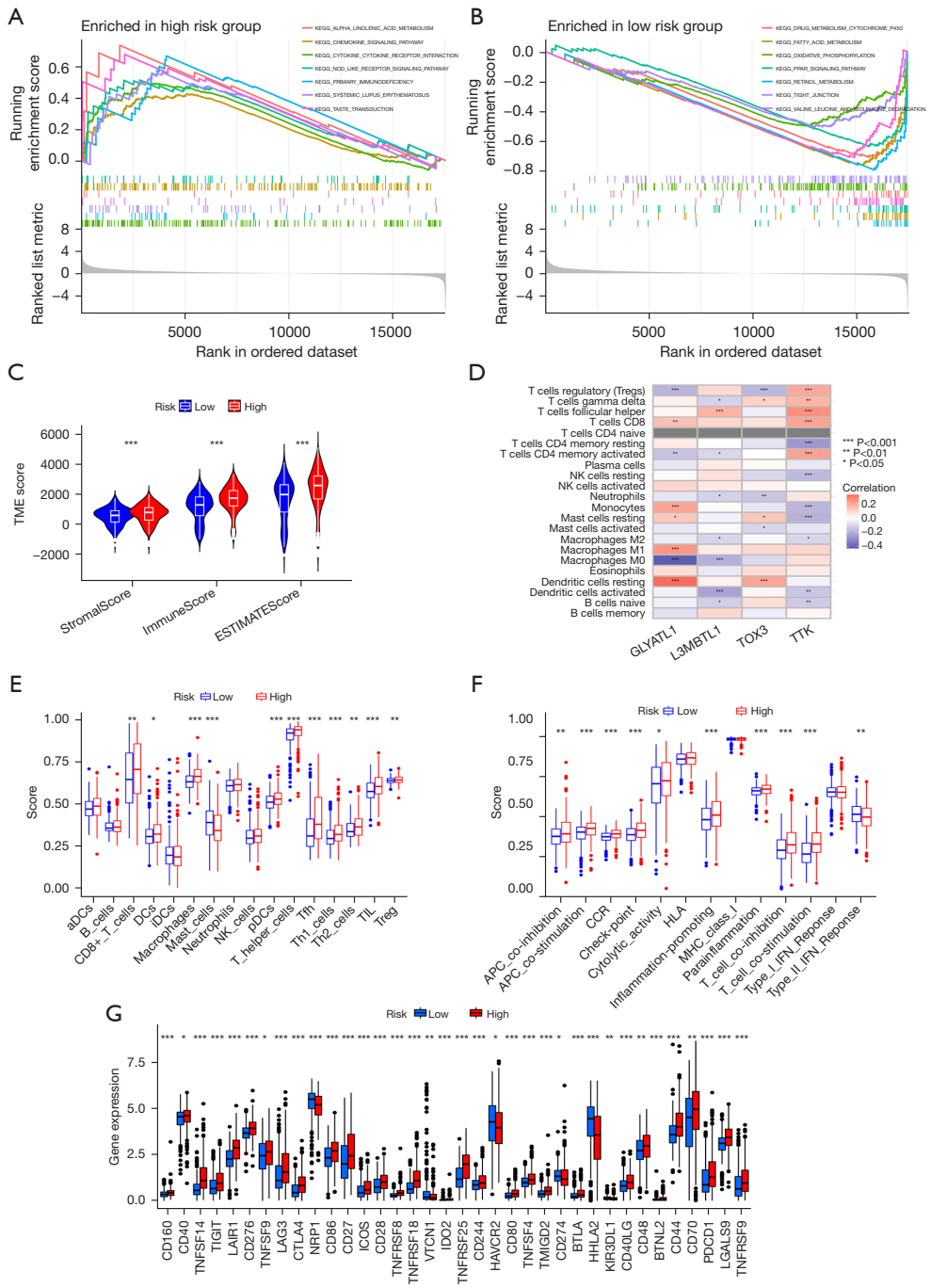

Figure 9 Functional enrichment analysis and immune characteristics between low- and high-risk groups. (A,B) The results of GSEA between the two groups. (C) Obvious difference in TME score between the two groups were observed according to the ESTIMATE algorithm. (D) The four CRs used to construct the model were closely related to most immune cells. (E,F) The differences in infiltration fractions of 16 human immune cells and the activity of 13 immune-related pathways between the two groups. (G) There were differences in the expression levels of 36 immune checkpoint genes between two groups. *, P<0.05; **, P<0.01; ***, P<0.001. KEGG, Kyoto Encyclopedia of Genes and Genomes; TME, tumor microenvironment; aDCs, activated dendritic cells; DCs, dendritic cells; iDC, immature dendritic cell; NK, natural killer; pDCs, plasmacytoid dendritic cells; Tfh, T follicular helper cells; TIL, tumor infiltrating lymphocytes; Treg, regulatory T cells; APC, antigen-presenting cells; CCR, C-C chemokine receptor; HLA, human leukocyte antigen; MHC, major histocompatibility complex; IFN, interferon; GSEA, Gene Set Enrichment Analysis; CRs, chromatin regulators.

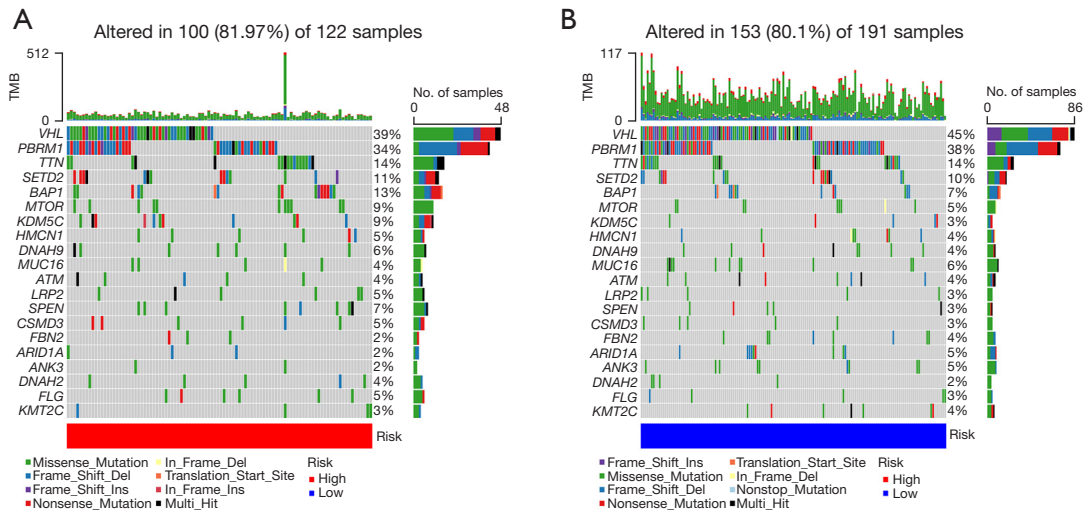

Figure 10 The waterfall diagram of the top 20 genes with the highest frequency of somatic mutation in the low- and high-risk group. (A) Distribution of somatic mutations in the high-risk group. (B) Distribution of somatic mutations in the low-risk group. TMB, tumor mutation burden.

Somatic mutation

Gene mutations is considered to be a vital factor in tumorigenesis and progression. Therefore, we analyzed the somatic mutation status among two groups. *Figure 10* shows the top 20 genes with the highest frequency of somatic mutation in two groups. Our results showed that missense mutation was the most popular type of somatic mutation in ccRCC, followed by frameshift deletion and nonsense mutation. The largest differences in mutations between groups were in VHL mutations, BAP1 mutations, and KDM5C mutations. Specifically, BAP1 mutations and KDM5C mutations were usual in the high-risk group (13% *vs.* 7%; 9% *vs.* 3%), while VHL mutations were popular in the low-risk group (45% *vs.* 39%).

Therapeutic response and drug sensitivity analysis

To improve the clinical value of CRs, we conducted a correlation analysis after acquiring and integrating data from the CellMiner platform (*Figure 11*). Cancer cells with higher mRNA levels of TTK may be more sensitive to nelarabine, but they may be associated with increased resistance to mithramycin. Higher expression levels of TOX3, cancer cells are more sensitive to LOXO-101, but they may be associated with increased resistance to pazopanib. Cancer cells with higher expression of GLYATL1 may be more sensitive to erlotinib, but it may be associated with increased resistance to vinorelbine and vinblastine. To improve the efficiency of clinical decision-making, we analyzed the drug sensitivity of two groups to common anticancer drugs. Higher IC50 values of lapatinib, AKT inhibitor VIII, and HER2 kinase inhibitor are observed in the high-risk group, suggesting patients with low-risk score were more sensitive to these drugs. While the IC50 values of vinblastine, gemcitabine, paclitaxel, axitinib, sunitinib, and temsirolimus were higher in the low-risk group, indicating patients with high-risk score may be more sensitive to these drugs (*Figure 12*).

Construction of a nomogram

In order to promote the clinical application of the risk model, we built a nomogram based on risk score and the patient's age, grade and AJCC stage. It contains four prognostic indicators, which can be better used to assess the survival probability of individuals in clinic (*Figure 13A*). The satisfied consistency between predicted and actual survival of patients can be observed from the calibration curve of the nomogram, confirming the superior predictive ability of the nomogram (*Figure 13B*).

Discussion

The ccRCC is a relatively special tumor. Unlike most tumors, its epigenetic regulators are frequently mutated

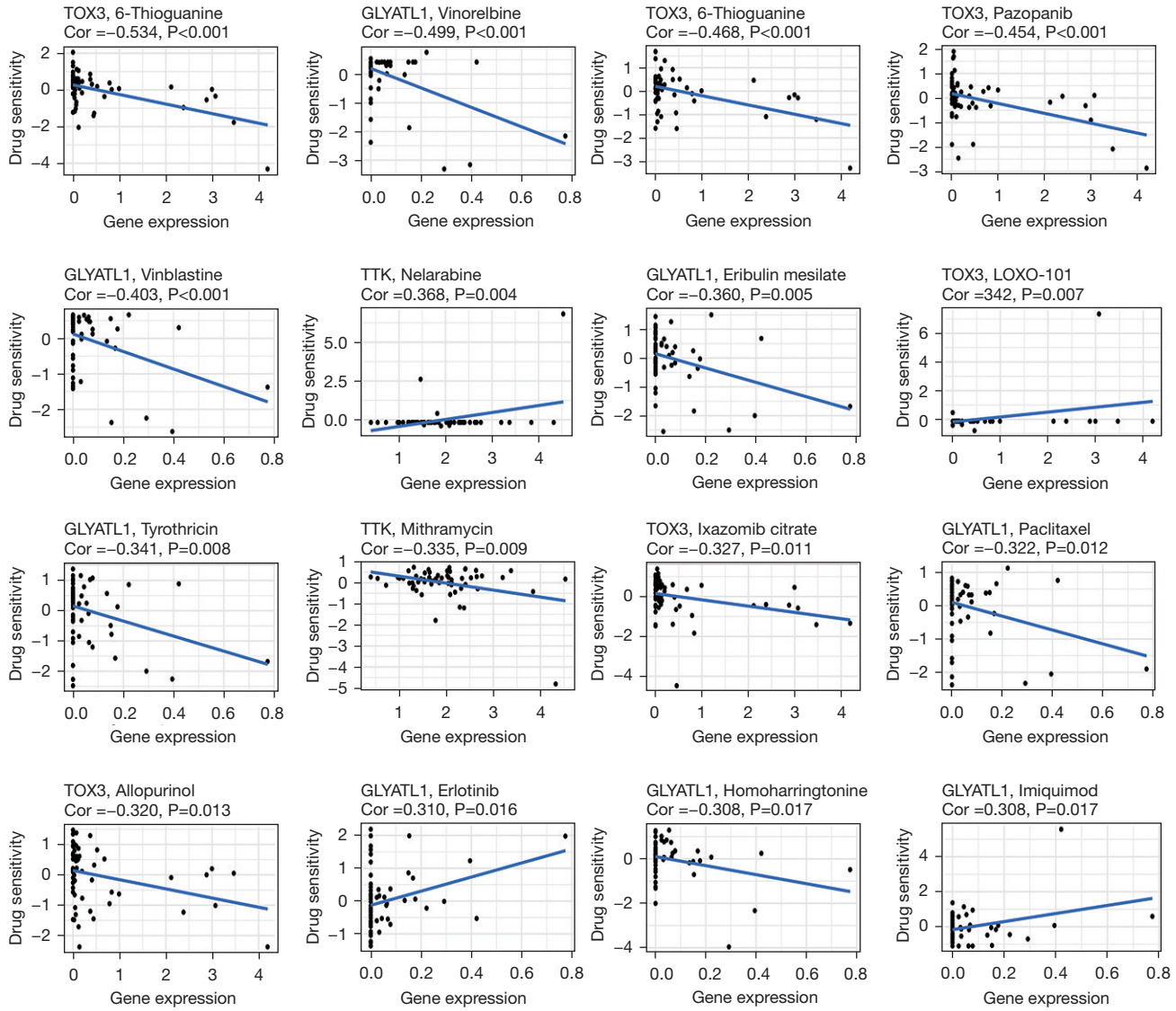

Figure 11 Correlation of CRs expressions with therapeutic response. CRs, chromatin regulators.

(such as SETD2, PBRM1, and BAP1), while gene pathways mutations in other common cancers (such as RAS, BRAF, and TP53) are largely absent (44-47). Previous studies (48) have demonstrated that inactivation of the VHL is a tumor-initiating incident in ccRCC, while the epigenetic expansion of VHL-HIF signaling output was considered to be a key link in driving multiple organ metastasis in RCC (49). These evidences suggest that epigenetic alterations are strongly related to the tumorigenesis and progression of ccRCC. However, how CRs drive epigenetic alterations function in ccRCC and their impacts on prognosis remain unclear.

In this research, we firstly identified 89 differentially expressed CRs between ccRCC and normal renal tissue in TCGA database and constructed their PPI network. Among them, TTK, TOP2A, BUB1, AURKB, and PBK are at the core of the network. At the same time, we also identified 60 differentially expressed TFs, and constructed a regulatory network between TFs and CRs. Thirty-three CRs were related with the prognosis of ccRCC, indicating that CRs may play a vital effect in tumorigenesis and progression of ccRCC. Based on 89 differentially expressed CRs, we executed an unsupervised clustering analysis of ccRCC patients in TCGA dataset and finally identified three subtypes. Obvious differences in CRs expression,

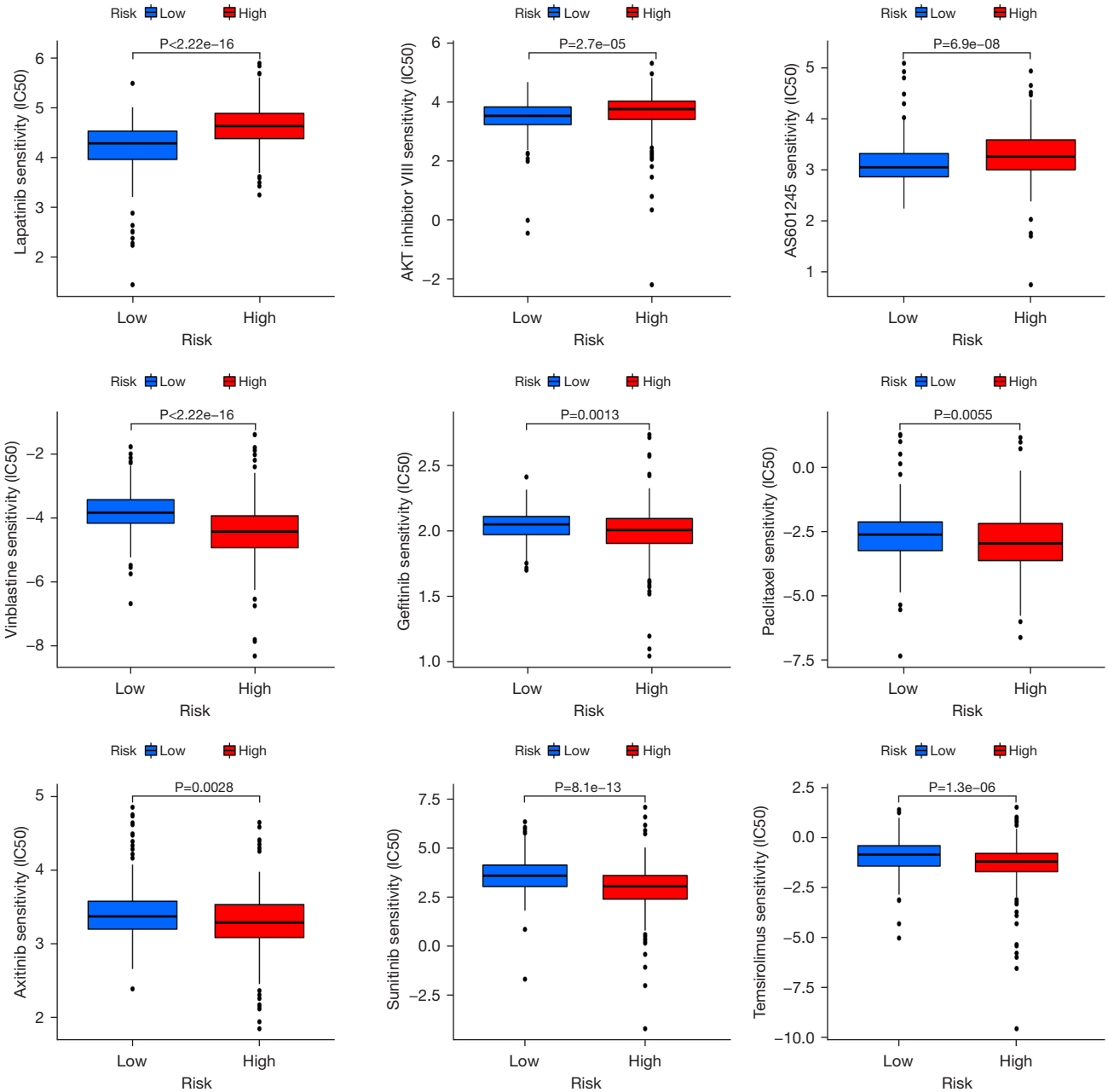

Figure 12 Differences in drug sensitivity between low- and high-risk group.

OS, PFS, and clinical features among the three subtypes were found. Compared with the other two subtypes, the overall expression of CRs in patients with subtype C2 was higher, while OS and PFS were shorter. In addition, subtype C2 was more common in men and was associated with poor histological grade, AJCC stage and TNM stage. Functional enrichment analysis was conducted to further research on the biological function differences of CRs in different subtypes. We discovered some immune-related biological processes and cancer-related signaling pathways, such as lymphocyte-mediated immunity, B cell-mediated immunity, complement activation; cytokine-cytokine receptor interaction, cell cycle, p53 signaling pathway, etc. The immune effects mediated by immune

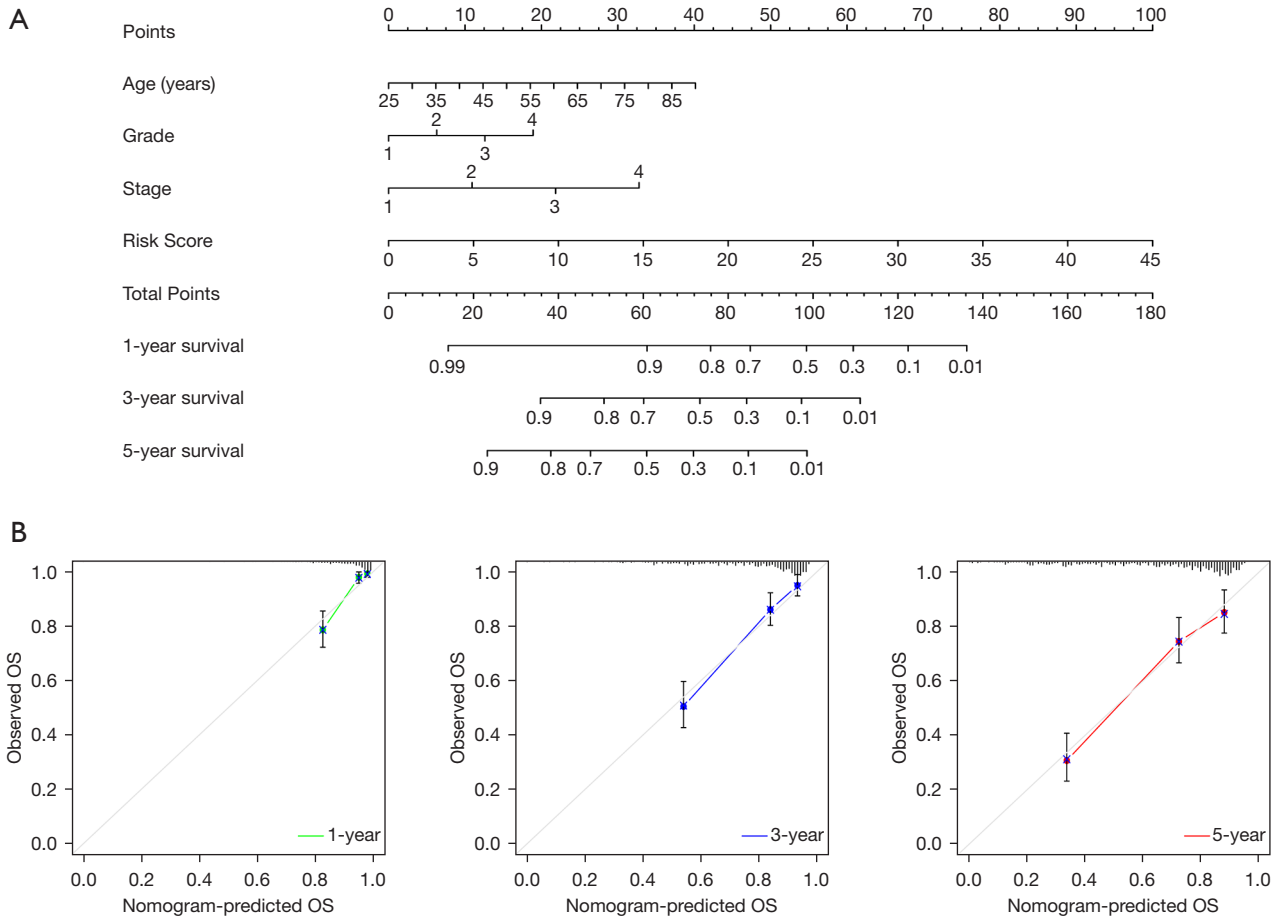

Figure 13 Construction of a nomogram for predicting survival. (A) A nomogram combining the clinical features and risk score was constructed to predict 1-, 3-, and 5-year OS. (B) The calibration curve of the nomogram showed excellent consistency between the actual and predicted survival of the patients. OS, overall survival.

cells can affect the progression of tumor. Li *et al.* (50) found that B cells recruited by tumor can significantly increase the invasive and metastatic ability of RCC. Ou *et al.* (51) found that regulation of IL-8 by B cells in the TME through mediated immune effects increased bladder cancer metastasis. In addition, inflammatory cytokines mediated by B cells were strongly associated with progression of colorectal cancer (52). P53 is mainly involved in biological processes such as cell cycle arrest, senescence, DNA repair, apoptosis, etc. In recent years, researchers have found that p53 is also involved in many other pathways, such as autophagy, cellular metabolism, ferroptosis, and pathways in metabolism of reactive oxygen species (53). The dysregulation of p53 signaling pathway and cell cycle may lead to the occurrence of many diseases including tumors. These evidences indicate that these biological processes and related pathways identified from CR-related subtypes are of great significance, revealing the possible potential mechanisms of CRs in the occurrence and progression of ccRCC.

Subsequently, we identified four CRs (TTK, L3MBTL1, GLYATL, and TOX3) with independent prognostic value by performing a multivariate Cox regression analysis. We successfully constructed a risk prognostic model using these four CRs. Survival curves and ROC curves showed the excellent predictive performance of the model and the model was validated in internal and external datasets. TTK is essential for the regulation of mitosis and chromosome attachment (54). It has been reported that TTK contributes greatly to the tumorigenesis and progression of many tumors (55-57). Zhang *et al.* (58) reported that TTK promoted cancer cell proliferation in colon cancer by

activating PKCα/ERK1/2 pathway and inhibited tumor differentiation by inactivating PI3K/Akt pathway. Huang *et al.* (54) reported that TTK can regulate cancer cells' apoptosis and proliferation by the Akt-mTOR signaling pathway in gastric cancer and silence of TTK inhibits tumor cell proliferation and increases apoptosis. Another study also showed that TTK can activate the Akt-mTOR signaling pathway in a p53-dependent manner, thereby promoting the proliferation and migration of hepatoma cells (59). Furthermore, Liu *et al.* (60) found that highly expressed in ccRCC tissues, TTK can promote tumor growth and metastasis via inducing cell proliferation and invasion. In mammals, L3MBTL1 was shown to be a transcriptional repressor and a suspected tumor suppressor gene (61). L3MBTL1 interacts with Tel/Etv6 and participates in the regulation of hematopoiesis in adults (62). L3MBTL may be the key gene of q12 deletion on chromosome 20 in human myeloid malignant tumors (63). However, no mutation of L3MBTL has been identified in patients with 20q deletion or in patients with normal cytogenetics (64). Gurvich *et al.* (65) suggested that 20q(-) hematopoietic malignancies develop as a result of replication stress and DNA damage caused by loss of L3MBTL1 expression. Highly expressed in breast cancer, L3MBTL1 was related to low histological grade and hormone receptor positivity, which contributes to good prognosis (61). GLYATL1, a member of the GLYATL gene family, is located in mitochondria and encodes an enzyme involved in catalyzing aryl acetyl transfer (66). Studies have shown that GLYATL1 is involved in many physiological metabolism, but is also associated with tumors. Guan *et al.* (67) found that high levels of promoter methylation of the GLYATL1 may silence the expression of GLYATL1, which leads to the occurrence of hepatocellular cancer and poor OS. Another research reported that GLYATL1 was up-expressed in primary prostate cancer and was regulated by the ETS TF ETV1 (68). As a member of the TOX gene family, TOX3 is abnormally expressed or mutated in malignant tumors. The TOX3 expression in mammary epithelial cell progenitors may lead to tumorigenesis of breast cancer (69). The up-regulation of TOX3 was observably related to the PFS and OS of lung adenocarcinoma (70). Besides, TOX3 is also considered to be a tumor suppressor gene, and the up-expressed of TOX3 inhibits the migration and invasion of ccRCC (71). This evidence suggests that the four CRs we identified may be potential therapeutic targets for many tumors, including ccRCC. Interestingly, we verified the expression level of the four CRs by high-throughput sequencing of tumor specimens. The results of univariate and multivariate Cox analyses also demonstrated that risk score constructed by four CRs can independently predict survival outcomes in ccRCC.

More and more evidences show the importance of TME in tumorigenesis, development and metastasis. Our findings revealed a momentous difference in TME between low- and high-risk group. Patients with high-risk score had higher immune score and stromal score, indicating higher levels of immune cells and stromal cells. The results of the ssGSEA demonstrated that patients with high-risk score generally had higher levels of immune cell infiltration and immune pathway activity, which was similar to known research (72). However, the high-risk group had a worse prognosis, indicating the complexity of the microenvironment in ccRCC. On the one hand, ccRCC may have a special immunophenotype. Although it possesses many immune cells, these cells cannot penetrate into the tumor cell nucleus, but are confined to the peripheral stroma of the tumor cell (73). On the other hand, immune cells in the microenvironment can be induced by various signaling pathways to become dysfunctional (74-76). Based on the above reasons, immune cells cannot exert the effect of killing tumors. The result of correlation analysis showed that the four CRs used to construct the model were obviously associated with most immune cells. In addition, we also observed that 36 immune checkpoints were differently expressed between two groups, including CTLA-4, LAG3, PD-1 and PD-L1, etc. Thus, we speculate it may also be a vital factor for the bad prognosis of high-risk group. Some new researches reported the interaction between cancer cell metabolism and immune cell metabolism can regulate anti-tumor immunity and affect the efficacy of immunotherapy (77). One of the characteristics of ccRCC is the mutation of target genes involved in metabolic pathways (78), thereby exhibiting distinct metabolic patterns. We found that CR-based gene signatures were enriched in cancer and metabolic-related pathways, such as NOD-like receptor signaling pathway, PPAR signaling pathway, chemokine signaling pathway; alpha linolenic acid metabolism, drug metabolism cytochrome p450, fatty acid metabolism, oxidative phosphorylation, valine leucine, and isoleucine degradation. Based on the above evidence, we speculate that CRs may decide tumor progression by affecting the immune signature and metabolic pattern of the TME. This suggests that targeting CRs may regulate the TME, enhance the efficacy of immunotherapy, and become a new therapeutic strategy.

To improve the value of CR-related prognostic model in clinical decision-making, we explored the relationship between CRs and the sensitivity of general anticancer drugs. Cancer cells with high expression of TOX3 may be more sensitive to LOXO-101. According to a study, LOXO-101 has a considerable effect on patients with advanced solid tumors that harbour an *NTRK* gene fusion (79). Tyrosine kinase inhibitors are commonly used drugs for the treatment of ccRCC. However, up-regulation of TOX3 may increase resistance to pazopanib. Cancer cells with high GLYATL1 expression may be more sensitive to erlotinib. Erlotinib induces cell cycle arrest by inhibiting epidermal growth factor receptor (EGFR), which prevents tumor cell division, and initiates programmed cell death in human tumor cells with overexpression of EGFR (80). However, the increased expression of GLYATL1 may increase drug resistance of vinorelbine and vinblastine. In addition, we found that patients with high-risk score may be more sensitive to vincristine, gemcitabine, paclitaxel, axitinib, sunitinib, and temsirolimus. This information can provide an important reference for clinical decision-making. Finally, we integrated the patient's clinical information and the risk score to develop a nomogram, which can better apply in clinical setting.

We have to admit that there are some limitations in our research. Firstly, the data we analyzed were from public databases, which need to be verified in forward-looking queue. Secondly, the risk prognostic model also needs to verify its predictive performance in more ccRCC cohorts. Finally, more researches are needed to explore the specific mechanism of CRs affecting the biological behavior of ccRCC.

Conclusions

Our research revealed the important role of CRs in the occurrence and development of ccRCC. The CR-related gene signature can predict the prognosis and drugs therapeutic significance of ccRCC, which provides an important reference for clinical decision-making. Targeting CRs may be a potential strategy for the treatment of ccRCC in the future.

Acknowledgments

We acknowledge the TCGA, ArrayExpress, MSigDB and Cistrome Cancer databases for providing available information.

Funding: This research was supported by the Medical Science and Technology Research Foundation of Guangdong Province (grant No. A2022232), and Foshan Nanhai District "14th Five-Year Plan" key specialty (special specialty) construction project.

Footnote

Reporting Checklist: The authors have completed the TRIPOD reporting checklist. Available at https://tcr.amegroups.com/article/view/10.21037/tcr-23-1383/rc

Data Sharing Statement: Available at https://tcr.amegroups.com/article/view/10.21037/tcr-23-1383/dss

Peer Review File: Available at https://tcr.amegroups.com/article/view/10.21037/tcr-23-1383/prf

Conflicts of Interest: All authors have completed the ICMJE uniform disclosure form (available at https://tcr.amegroups.com/article/view/10.21037/tcr-23-1383/coif). The authors have no conflicts of interest to declare.

Ethical Statement: The authors are accountable for all aspects of the work in ensuring that questions related to the accuracy or integrity of any part of the work are appropriately investigated and resolved. The study was conducted in accordance with the Declaration of Helsinki (as revised in 2013). The study was approved by the Ethics Committee of Guangdong Provincial People's Hospital (IRB No. KY-Z-2021-657-01) and informed consent was obtained from all individual participants.

References

1. Siegel RL, Miller KD, Fuchs HE, et al. Cancer statistics, 2022. CA Cancer J Clin 2022;72:7-33.
2. Sung H, Ferlay J, Siegel RL, et al. Global Cancer Statistics

2020: GLOBOCAN Estimates of Incidence and Mortality Worldwide for 36 Cancers in 185 Countries. CA Cancer J Clin 2021;71:209-49.
3. Hsieh JJ, Purdue MP, Signoretti S, et al. Renal cell carcinoma. Nat Rev Dis Primers 2017;3:17009.
4. Kim MC, Jin Z, Kolb R, et al. Updates on Immunotherapy and Immune Landscape in Renal Clear Cell Carcinoma. Cancers (Basel) 2021;13:5856.
5. Yang F, Zhou Q, Xing N. Comparison of survival and renal function between partial and radical laparoscopic nephrectomy for T1b renal cell carcinoma. J Cancer Res Clin Oncol 2020;146:261-72.
6. Barata PC, Rini BI. Treatment of renal cell carcinoma: Current status and future directions. CA Cancer J Clin 2017;67:507-24.
7. McKay RR, Bossé D, Xie W, et al. The Clinical Activity of PD-1/PD-L1 Inhibitors in Metastatic Non-Clear Cell Renal Cell Carcinoma. Cancer Immunol Res 2018;6:758-65.
8. Choueiri TK, Motzer RJ. Systemic Therapy for Metastatic Renal-Cell Carcinoma. N Engl J Med 2017;376:354-66.
9. Miller KD, Nogueira L, Mariotto AB, et al. Cancer treatment and survivorship statistics, 2019. CA Cancer J Clin 2019;69:363-85.
10. Motzer RJ, Escudier B, McDermott DF, et al. Nivolumab versus Everolimus in Advanced Renal-Cell Carcinoma. N Engl J Med 2015;373:1803-13.
11. Chen J, Ye Z, Liu L, et al. Assessment of the prognostic value of SPOCK1 in clear cell renal cell carcinoma: a bioinformatics analysis. Transl Androl Urol 2022;11:509-18.
12. Shao Y, Wu B, Yang Z, et al. ALDOB represents a potential prognostic biomarker for patients with clear cell renal cell carcinoma. Transl Androl Urol 2023;12:549-71.
13. Liao Z, Yao H, Wei J, et al. Development and validation of the prognostic value of the immune-related genes in clear cell renal cell carcinoma. Transl Androl Urol 2021;10:1607-19.
14. Zhou Y, Jiang D, Chu X, et al. High expression of CD73 contributes to poor prognosis of clear-cell renal cell carcinoma by promoting cell proliferation and migration. Transl Cancer Res 2022;11:3634-44.
15. Brien GL, Valerio DG, Armstrong SA. Exploiting the Epigenome to Control Cancer-Promoting Gene-Expression Programs. Cancer Cell 2016;29:464-76.
16. Lu J, Xu J, Li J, et al. FACER: comprehensive molecular and functional characterization of epigenetic chromatin regulators. Nucleic Acids Res 2018;46:10019-33.
17. Plass C, Pfister SM, Lindroth AM, et al. Mutations in regulators of the epigenome and their connections to global chromatin patterns in cancer. Nat Rev Genet 2013;14:765-80.
18. Gonzalez-Perez A, Jene-Sanz A, Lopez-Bigas N. The mutational landscape of chromatin regulatory factors across 4,623 tumor samples. Genome Biol 2013;14:r106.
19. Medvedeva YA, Lennartsson A, Ehsani R, et al. EpiFactors: a comprehensive database of human epigenetic factors and complexes. Database (Oxford) 2015;2015:bav067.
20. Marazzi I, Greenbaum BD, Low DHP, et al. Chromatin dependencies in cancer and inflammation. Nat Rev Mol Cell Biol 2018;19:245-61.
21. Chu Y, Chen W, Peng W, et al. Amnion-Derived Mesenchymal Stem Cell Exosomes-Mediated Autophagy Promotes the Survival of Trophoblasts Under Hypoxia Through mTOR Pathway by the Downregulation of EZH2. Front Cell Dev Biol 2020;8:545852.
22. Li T, Yang J, Yang B, et al. Ketamine Inhibits Ovarian Cancer Cell Growth by Regulating the lncRNA-PVT1/EZH2/p57 Axis. Front Genet 2021;11:597467.
23. Chen J, Wang F, Xu H, et al. Long Non-Coding RNA SNHG1 Regulates the Wnt/β-Catenin and PI3K/AKT/mTOR Signaling Pathways via EZH2 to Affect the Proliferation, Apoptosis, and Autophagy of Prostate Cancer Cell. Front Oncol 2020;10:552907.
24. Cancer Genome Atlas Research Network, Ley TJ, Miller C, et al. Genomic and epigenomic landscapes of adult de novo acute myeloid leukemia. N Engl J Med 2013;368:2059-74.
25. Shain AH, Pollack JR. The spectrum of SWI/SNF mutations, ubiquitous in human cancers. PLoS One 2013;8:e55119.
26. Alizadeh AA, Aranda V, Bardelli A, et al. Toward understanding and exploiting tumor heterogeneity. Nat Med 2015;21:846-53.
27. Banelli B, Carra E, Barbieri F, et al. The histone demethylase KDM5A is a key factor for the resistance to temozolomide in glioblastoma. Cell Cycle 2015;14:3418-29.
28. Sharma SV, Lee DY, Li B, et al. A chromatin-mediated reversible drug-tolerant state in cancer cell subpopulations. Cell 2010;141:69-80.
29. Fiorentino FP, Giordano A. The tumor suppressor role of CTCF. J Cell Physiol 2012;227:479-92.
30. Marshall AD, Bailey CG, Rasko JE. CTCF and BORIS in genome regulation and cancer. Curr Opin Genet Dev 2014;24:8-15.
31. Damaschke NA, Yang B, Blute ML Jr, et al. Frequent disruption of chromodomain helicase DNA-binding

protein 8 (CHD8) and functionally associated chromatin regulators in prostate cancer. Neoplasia 2014;16:1018-27.
32. Huang Z, Yan Y, Zhu Z, et al. CBX7 suppresses urinary bladder cancer progression via modulating AKR1B10-ERK signaling. Cell Death Dis 2021;12:537.
33. Shinjo K, Yamashita Y, Yamamoto E, et al. Expression of chromobox homolog 7 (CBX7) is associated with poor prognosis in ovarian clear cell adenocarcinoma via TRAIL-induced apoptotic pathway regulation. Int J Cancer 2014;135:308-18.
34. Li Z, Hou P, Fan D, et al. The degradation of EZH2 mediated by lncRNA ANCR attenuated the invasion and metastasis of breast cancer. Cell Death Differ 2017;24:59-71.
35. Zhang L, Qu J, Qi Y, et al. EZH2 engages TGFβ signaling to promote breast cancer bone metastasis via integrin β1-FAK activation. Nat Commun 2022;13:2543.
36. Yang YA, Yu J. EZH2, an epigenetic driver of prostate cancer. Protein Cell 2013;4:331-41.
37. White JR, Thompson DT, Koch KE, et al. AP-2α-Mediated Activation of E2F and EZH2 Drives Melanoma Metastasis. Cancer Res 2021;81:4455-70.
38. Roh JW, Choi JE, Han HD, et al. Clinical and biological significance of EZH2 expression in endometrial cancer. Cancer Biol Ther 2020;21:147-56.
39. Cai H, Memarzadeh S, Stoyanova T, et al. Collaboration of Kras and androgen receptor signaling stimulates EZH2 expression and tumor-propagating cells in prostate cancer. Cancer Res 2012;72:4672-81.
40. Yue X, Zhang Z, Liang X, et al. Zinc fingers and homeoboxes 2 inhibits hepatocellular carcinoma cell proliferation and represses expression of Cyclins A and E. Gastroenterology 2012;142:1559-70.e2.
41. Kwon RJ, Kim YH, Jeong DC, et al. Expression and prognostic significance of zinc fingers and homeoboxes family members in renal cell carcinoma. PLoS One 2017;12:e0171036.
42. Lyu XY, Shui YS, Wang L, et al. WDR5 promotes the tumorigenesis of oral squamous cell carcinoma via CARM1/β-catenin axis. Odontology 2022;110:138-47.
43. Lu C, Liu Z, Klement JD, et al. WDR5-H3K4me3 epigenetic axis regulates OPN expression to compensate PD-L1 function to promote pancreatic cancer immune escape. J Immunother Cancer 2021;9:e002624.
44. Simon JM, Hacker KE, Singh D, et al. Variation in chromatin accessibility in human kidney cancer links H3K36 methyltransferase loss with widespread RNA processing defects. Genome Res 2014;24:241-50.
45. Comprehensive molecular characterization of clear cell renal cell carcinoma. Nature 2013;499:43-9.
46. Dalgliesh GL, Furge K, Greenman C, et al. Systematic sequencing of renal carcinoma reveals inactivation of histone modifying genes. Nature 2010;463:360-3.
47. Duns G, van den Berg E, van Duivenbode I, et al. Histone methyltransferase gene SETD2 is a novel tumor suppressor gene in clear cell renal cell carcinoma. Cancer Res 2010;70:4287-91.
48. Kaelin WG Jr. The von Hippel-Lindau tumour suppressor protein: O2 sensing and cancer. Nat Rev Cancer 2008;8:865-73.
49. Vanharanta S, Shu W, Brenet F, et al. Epigenetic expansion of VHL-HIF signal output drives multiorgan metastasis in renal cancer. Nat Med 2013;19:50-6.
50. Li S, Huang C, Hu G, et al. Tumor-educated B cells promote renal cancer metastasis via inducing the IL-1β/HIF-2α/Notch1 signals. Cell Death Dis 2020;11:163. Erratum in: Cell Death Dis 2022;13:415.
51. Ou Z, Wang Y, Liu L, et al. Tumor microenvironment B cells increase bladder cancer metastasis via modulation of the IL-8/androgen receptor (AR)/MMPs signals. Oncotarget 2015;6:26065-78.
52. Lasry A, Zinger A, Ben-Neriah Y. Inflammatory networks underlying colorectal cancer. Nat Immunol 2016;17:230-40.
53. Hernández Borrero LJ, El-Deiry WS. Tumor suppressor p53: Biology, signaling pathways, and therapeutic targeting. Biochim Biophys Acta Rev Cancer 2021;1876:188556.
54. Huang H, Yang Y, Zhang W, et al. TTK regulates proliferation and apoptosis of gastric cancer cells through the Akt-mTOR pathway. FEBS Open Bio 2020;10:1542-9.
55. Benzi G, Camasses A, Atsunori Y, et al. A common molecular mechanism underlies the role of Mps1 in chromosome biorientation and the spindle assembly checkpoint. EMBO Rep 2020;21:e50257.
56. Silva RD, Mirkovic M, Guilgur LG, et al. Absence of the Spindle Assembly Checkpoint Restores Mitotic Fidelity upon Loss of Sister Chromatid Cohesion. Curr Biol 2018;28:2837-2844.e3.
57. Lim G, Huh WK. Rad52 phosphorylation by Ipl1 and Mps1 contributes to Mps1 kinetochore localization and spindle assembly checkpoint regulation. Proc Natl Acad Sci U S A 2017;114:E9261-70.
58. Zhang L, Jiang B, Zhu N, et al. Mitotic checkpoint kinase Mps1/TTK predicts prognosis of colon cancer patients and regulates tumor proliferation and differentiation via PKCα/ERK1/2 and PI3K/Akt pathway. Med Oncol 2019;37:5.

59. Liu X, Liao W, Yuan Q, et al. TTK activates Akt and promotes proliferation and migration of hepatocellular carcinoma cells. Oncotarget 2015;6:34309-20.
60. Liu XD, Yao DW, Xin F. TTK contributes to tumor growth and metastasis of clear cell renal cell carcinoma by inducing cell proliferation and invasion. Neoplasma 2019;66:946-53.
61. Zeng H, Irwin ML, Lu L, et al. Physical activity and breast cancer survival: an epigenetic link through reduced methylation of a tumor suppressor gene L3MBTL1. Breast Cancer Res Treat 2012;133:127-35.
62. Hock H, Meade E, Medeiros S, et al. Tel/Etv6 is an essential and selective regulator of adult hematopoietic stem cell survival. Genes Dev 2004;18:2336-41.
63. Li J, Bench AJ, Vassiliou GS, et al. Imprinting of the human L3MBTL gene, a polycomb family member located in a region of chromosome 20 deleted in human myeloid malignancies. Proc Natl Acad Sci U S A 2004;101:7341-6.
64. MacGrogan D, Kalakonda N, Alvarez S, et al. Structural integrity and expression of the L3MBTL gene in normal and malignant hematopoietic cells. Genes Chromosomes Cancer 2004;41:203-13.
65. Gurvich N, Perna F, Farina A, et al. L3MBTL1 polycomb protein, a candidate tumor suppressor in del(20q12) myeloid disorders, is essential for genome stability. Proc Natl Acad Sci U S A 2010;107:22552-7.
66. Barfeld SJ, East P, Zuber V, et al. Meta-analysis of prostate cancer gene expression data identifies a novel discriminatory signature enriched for glycosylating enzymes. BMC Med Genomics 2014;7:513.
67. Guan R, Hong W, Huang J, et al. The expression and prognostic value of GLYATL1 and its potential role in hepatocellular carcinoma. J Gastrointest Oncol 2020;11:1305-21.
68. Eich ML, Chandrashekar DS, Rodriguez Pen A MDC, et al. Characterization of glycine-N-acyltransferase like 1 (GLYATL1) in prostate cancer. Prostate 2019;79:1629-39.
69. Seksenyan A, Kadavallore A, Walts AE, et al. TOX3 is expressed in mammary ER(+) epithelial cells and regulates ER target genes in luminal breast cancer. BMC Cancer 2015;15:22.
70. Zeng D, Lin H, Cui J, et al. TOX3 is a favorable prognostic indicator and potential immunomodulatory factor in lung adenocarcinoma. Oncol Lett 2019;18:4144-52.
71. Jiang B, Chen W, Qin H, et al. TOX3 inhibits cancer cell migration and invasion via transcriptional regulation of SNAI1 and SNAI2 in clear cell renal cell carcinoma. Cancer Lett 2019;449:76-86.
72. Newman AM, Liu CL, Green MR, et al. Robust enumeration of cell subsets from tissue expression profiles. Nat Methods 2015;12:453-7.
73. Chen DS, Mellman I. Elements of cancer immunity and the cancer-immune set point. Nature 2017;541:321-30.
74. Prinz PU, Mendler AN, Brech D, et al. NK-cell dysfunction in human renal carcinoma reveals diacylglycerol kinase as key regulator and target for therapeutic intervention. Int J Cancer 2014;135:1832-41.
75. Xia Y, Zhang Q, Zhen Q, et al. Negative regulation of tumor-infiltrating NK cell in clear cell renal cell carcinoma patients through the exosomal pathway. Oncotarget 2017;8:37783-95.
76. Giraldo NA, Becht E, Pagès F, et al. Orchestration and Prognostic Significance of Immune Checkpoints in the Microenvironment of Primary and Metastatic Renal Cell Cancer. Clin Cancer Res 2015;21:3031-40.
77. Leone RD, Powell JD. Metabolism of immune cells in cancer. Nat Rev Cancer 2020;20:516-31.
78. Lucarelli G, Loizzo D, Franzin R, et al. Metabolomic insights into pathophysiological mechanisms and biomarker discovery in clear cell renal cell carcinoma. Expert Rev Mol Diagn 2019;19:397-407.
79. Hong DS, DuBois SG, Kummar S, et al. Larotrectinib in patients with TRK fusion-positive solid tumours: a pooled analysis of three phase 1/2 clinical trials. Lancet Oncol 2020;21:531-40.
80. Abdelgalil AA, Al-Kahtani HM, Al-Jenoobi FI. Erlotinib. Profiles Drug Subst Excip Relat Methodol 2020;45:93-117.

Cite this article as: Zhang C, Zeng J, Ye C, Tian K, Xian Z. Construction and validation of a chromatin regulator-related gene signature for prognostic and therapeutic significance of clear cell renal cell carcinoma. Transl Cancer Res 2024;13(1):150-172. doi: 10.21037/tcr-23-1383

